

Synthesis and photocatalytic dye degradation properties of Zinc Oxide-Tin (IV) antimonophosphatenanocomposite ion exchanger

Mandeep Kaur¹, Sandeep Kaushal^{1*} and Pritpal Singh^{1*}

¹ Department of Chemistry,

Sri Guru Granth Sahib World University, Fatehgarh Sahib, Punjab, (India)

ABSTRACT

The sol-gel method is used to synthesize Zinc Oxide- Tin (IV) antimonophosphate (ZnO/SnSbP) nanocomposite. Analytical techniques such as scanning electron microscopy (SEM), transmission electron microscopy (TEM), X-ray diffraction (XRD) and fourier transform infrared spectroscopy (FTIR) are used for the characterization of the nanocomposite material. The nanocomposite ion exchanger is explored for its ion exchange capacity and a comparative analysis with an inorganic part is drawn. The degradation of Methylene blue (MB) dye has been studied by Zinc Oxide-Tin (IV) antimonophosphate ion exchanger as a photocatalyst in the aqueous medium. It is observed that the nanocomposite (ZnO/SnSbP) exchanger has shown excellent dye degradation efficiency.

Keywords: Ion Exchange Capacity, Nanocomposite Ion Exchanger, Photocatalyst

I. INTRODUCTION

Natural dyes obtained from natural resources as trees and plants (roots, bark, leaves, wood etc.) vegetables, minerals or invertebrates. It is recoverable, environment-friendly and sounder than synthetic dyes. However, widespread of synthetic dyes in textile industries are due to a huge variety of colour and long-lasting, in contrast, the drop of natural dyes because of yield, cost-effectiveness, synthesis process etc. Various industries like leather, food, cosmetics, electro winning, textiles, bleaching, pulp, pharmaceuticals, soap, detergent etc. used synthetic dyes and directly release dye effluents into an environment without using adequate remediation; it had adverse effects into marine ecosystem and human beings. In this way, there must be eliminated colour pollution before discharged into the water system [1-5]. Methylene blue (C₁₆H₁₈ClN₃S) is a basic dye with dark green crystal and gives deep blue colour in water solution and the side effect of MB dye is dizziness, nausea, headache, lungs and skin problems, hypertension and difficulty in breathing [6-8].

Multiple techniques have been adopted such as biological process, ozone treatments, advanced chemical oxidation, photocatalysis, membrane technologies, adsorption etc. for the deduction of organic waste effluents [9-13]. All of above, photocatalytic process is easy, fast degraded, and a most adept way for the degeneration of organic contaminants. Nanoparticles such as ZnO, GO, SnO₂, ZrO₂, TiO₂, Fe₂O₃ etc. have acted as dominant photocatalysts for decomposition and reaction medium for organic pollutants [14-17]. However, synthesizing of new nanocomposite ion exchangers have enhanced their mechanical, physical properties like

granularity, thermal and mechanical stability, selectivity, photocatalysis and magnificent ion exchange capacity. Composite ion exchangers mixed with nanoparticles have great captivation due to their good productivity in the photocatalytic process. In this photochemical reaction, an electron-hole pair is generated by the metal ions and participated in oxidation-reduction method and produce OH^{\bullet} and $\text{O}_2^{\bullet-}$ free radicals that resulted in degeneration of organic dye pollutants [18-21].

In this research, the sol-gel method is used for the formation of ZnO-SnSbP nanocomposite ion exchanger and analyzed with different techniques like SEM, FTIR, XRD, TEM and characteristics of exchanger material are explored. Heterogeneous catalysis of basic dye i.e. Methylene blue (MB) dyes in the solar region is exhibited great efficiency with ZnO-SnSbP nanocomposite.

II. EXPERIMENTAL

2.1. Materials and Methods

2.1.1. Reagents and instruments

Analytical grade tin (IV) chloride, phosphoric acid, potassium pyroantimonate, hydrochloric acid and hydrofluoric acid are used for the preparation of exchangers. All the reagents are prepared in double distilled water (DDW). FTIR spectra are showed on a Perkin Elmer RXIFIR spectrometer. X-ray diffraction structures are obtained using PAN analytical system DY 3190 X-ray diffractometer. The spectrum is recorded between 5° to 40° at 2θ , using $\text{CuK}\alpha$ radiation. The topography and elemental composition of the particles are displayed using Scanning electron microscopy (SEM) attached to an energy dispersive X-ray (EDX) spectrometer (HITACHI, SU8010 electron microscope). Transmission electron microscopy (TEM, Tecnai G2 20, 200KeV FEI) is used for the sample morphology and microstructure. The UV-Vis spectrometer is operated between 200-800 nm wavelengths (Model UV-2600, SHIMADZU copp 01197).

2.1.2. Synthesis of Zinc oxide-Tin (IV) antimonophosphate (ZnO-SnSbP) nanocomposite

The Zinc Oxide-tin (IV) antimonophosphate (ZnO-SnSbP) nanocomposite ion exchanger is synthesized by the sol-gel method. Tin (IV) chloride solution (0.1 M) is added to a continuously stirred mixture of potassium pyroantimonate (0.1 M) and phosphoric acid solutions (0.1 M) at 60°C , in the volume ratio 2:1:1. After complete addition, the mixture is stirred for 2 hours and a gel of tin (IV) antimonophosphate (SnSbP) is obtained. Zinc oxide nanoparticles are then added to tin (IV) antimonophosphate gel. The resultant mixture is stirred for 12 hours on a magnetic stirrer and then digested for 24 h with intermittent shaking. The precipitates are filtered and washed with double distilled water several times to remove the impurities. The precipitates of ZnO-SnSbP obtained are dried at 40°C in a hot air oven. The dried precipitates are converted into H^+ form by placing in 0.1 M HCl solution for 24 h with occasional shaking. The precipitates of ZnO-SnSbP are filtered and washed with distilled water to remove excess of acid. Seven samples (S1-S7) are prepared by varying the mixing volume ratio of Zinc oxide and tin (IV) antimonophosphate (ZnO-SnSbP) and determined their ion exchange capacity.

2.1.3. Ion exchange capacity

The sample ion exchange capacity (IEC) is measured before proceeding for further studies. Ion exchange capacity is discovered by method column operation using the solution of sodium nitrate as an eluent. The H⁺ ions rinsed from the column were found out titrimetrically towards a standard chemical solution of sodium hydroxide.

$$IEC = \frac{N \times V}{W} \text{ meq/g} \quad \dots (1)$$

In this, N and V are the normality and volume (mL), respectively of NaOH solution used and W is the mass of the ion exchanger in gram.

2.1.4. Photo catalysis

The ZnO-SnSbP nanocomposite ion exchange material as a photocatalyst is used for the degradation of methylene blue (MB) dye. The ZnO-SnSbP (25 mg) is added as a catalyst to 100 mL aqueous solution containing 1.6 mg of MB dye. The final solution in a beaker is remained in dark for an hour and stirred continuously to arrive at equilibrium. After that, the solution is kept in solar light and 2 ml sample solutions are withdrawn from the main solution after 30 min interval, centrifuged for 10 min and their absorbance is recorded at 664 nm for methylene blue dye using the UV-Vis spectrophotometer.

Degradation percentage for MB dye is calculated by the formula mention below [15]:

$$\text{Percentage of dye removal} = \frac{A_0 - A_t}{A_0} \times 100 \quad \dots (2)$$

where A₀ and A_t are the initial and final absorbance, respectively.

III. RESULTS AND DISCUSSION

Five different samples (S1-S5, Table 1) are synthesized by varying the volume ratio of inorganic exchanger and tin oxide nanoparticles. All the samples of nanocomposite are acquired better ion exchange capacity (IEC) toward Na⁺ ions than its inorganic part (SnSbP). Tin oxide in nano form united into the inorganic matrix raised the surface area and hence, increased the number of ion exchange sites in the exchanger. The sample S5 has better IEC of 1.65 meq g⁻¹ for Na⁺ ions as compared to 1.35 meq g⁻¹ of SnSbP and selected for further studies.

Table 1: Condition of Synthesis and Ion Exchange Capacity of Different Samples of ZnO/SnSbP A: Tin (IV) chloride; B: Potassium pyroantimonate; C: Phosphoric acid; D: ZnO

Sample No.	A (mol L ⁻¹)	B (mol L ⁻¹)	C (mol L ⁻¹)	Mixing ratio (v/v)	D (%)	IEC (meqg ⁻¹)
S1	0.1	0.1	0.1	2:1:1	0	1.35
S2	0.1	0.1	0.1	2:1:1	1	1.39
S3	0.1	0.1	0.1	2:1:1	2	1.40

S4	0.1	0.1	0.1	2:1:1	4	1.53
S5	0.1	0.1	0.1	2:1:1	6	1.65
S6	0.1	0.1	0.1	2:1:1	8	1.60
S7	0.1	0.1	0.1	2:1:1	10	1.50

3.1. Structural and morphological characterization of ZnO/SnSbPnanocomposite

3.1.1. Fourier Transform Infrared analysis

The FTIR spectra of ZnO, SnSbP and ZnO/SnSbP are displayed in Fig.1. The absorption stretching vibration of a metal-oxygen bond is observed in between 400-600 cm^{-1} . In (Fig 1a) the peak at 420.40 cm^{-1} is because of Zn-O stretching vibration modes [22] and asymmetric and symmetric stretching vibration of water molecules at 3411.4 cm^{-1} . However, the bending vibration of H-O-H group in water is observed at 1629.4 cm^{-1} . Vibration modes at 3448 and 3459.1 cm^{-1} and 1631.4 cm^{-1} are caused by the presence of crystallization of water in (Fig. 1b and c). The peak at 2441.4 and 2457.8 cm^{-1} is described to stretching modes of acidic O-H group. The band 1062.5 cm^{-1} and 1031.2 cm^{-1} are ascribed to stretching of P=O in phosphate (PO_4^{3-}) group. The band at 538.03 and 552.6 cm^{-1} are caused by Sn-O stretching vibrations [23, 24]. The absorption band at 416.14 cm^{-1} has supported the formation of nanosized ZnO particles in Fig. (1c) as there is no such peak in SnSbP. In Fig. (1c), it is remarked that there is a decline in the frequency and a small shift in the stretching mode of Zn-O and it shifted from 420 to 416.14 cm^{-1} . This can be described on the basis of Hooke's law [25] the vibration frequency is indirectly proportional to reduced mass i.e. as the addition of reduced mass (μ) leads to decrease in the vibrational frequency.

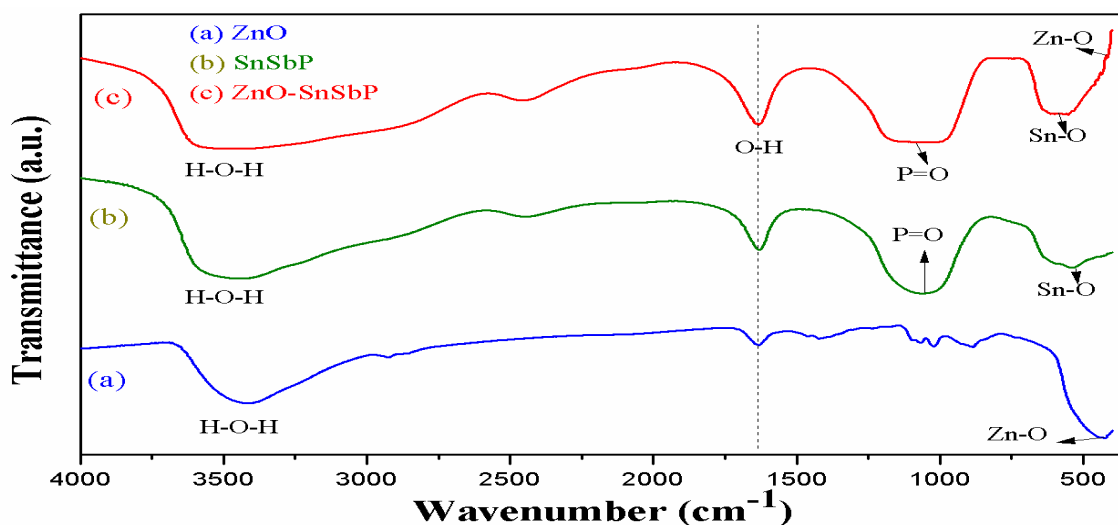


Fig.1. FTIR spectra of (a) ZnO, (b) SnSbP ion exchanger and (c) ZnO-SnSbPnanocomposite ion exchanger.

3.1.2. X-Ray diffraction studies

The diffraction peaks of ZnO are listed to the hexagonal structure and matched with the standard JCPDS Card No. 00-036-1451. The diffraction peaks at the diffraction angles of 31.7, 34.4, 36.3, 47.5, 56.6, 62.8, 66.4, 67.9, 69 are attributed to (100), (002), (101), (110), (103), (200), (112), (201) planes indicating the crystalline nature of ZnO and it has been further cross-checked with the literature [19]. The tin antimonophosphate (SnSbP) ion exchanger diffraction peaks angles and planes are assigned at 18.4(212), 23.4(213), 28.3(204) and matched with JCPDS card no.01-077-1929. In nanocomposite (ZnO-SnSbP) two peaks of ZnO showed at (101) and (110) planes and three peaks of SnSbP displayed. From this, it is confirmed that ZnO was incorporated with SnSbP ion exchanger.

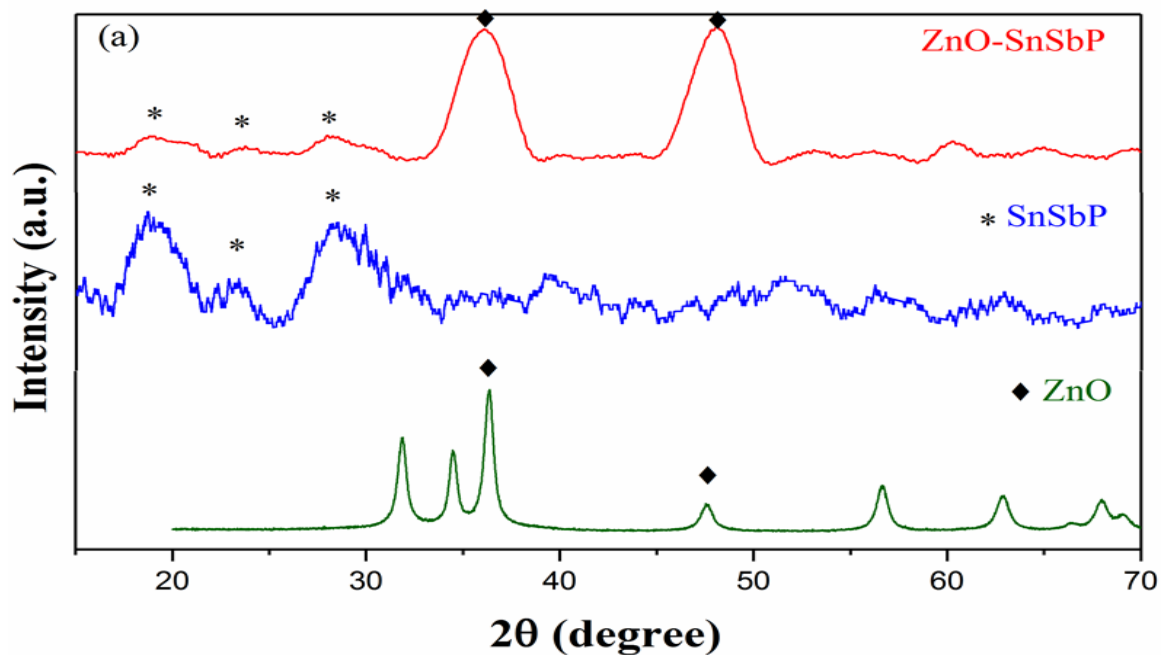


Fig.2.X-Ray diffraction pattern of (a)ZnO,SnSbP and ZnO-SnSbP

3.1.3. Field Emission Scanning Electron Microscopy and Energy Dispersive X-ray studies

Field emission scanning electron images of ZnO, SnSbP and ZnO/SnSbP have appeared in Fig.3 (a, b and c). The results of ZnO/SnSbP proved that the morphology has changed after incorporation of Zinc oxide nanoparticles with inorganic components in nanocomposite material. In the FESEM micrograph, the spherical shape in grey appearance can be due to SnSbP layer and the triangular shape in white can be represented the ZnO nanoparticles. The nanocomposite may be agglomerated and irregular in shape. Thus peaks in EDX spectrum of ZnO/SnSbP nanocomposite (Fig. 3d) is confirmed the existence of Sn, O, Sb, P, Zn elements and in the inset (Fig. 3d) the atomic percentage of Zn:Sn:Sb:P:O is calculated to be 0.47:7.25:0.21:7.55:84.53.

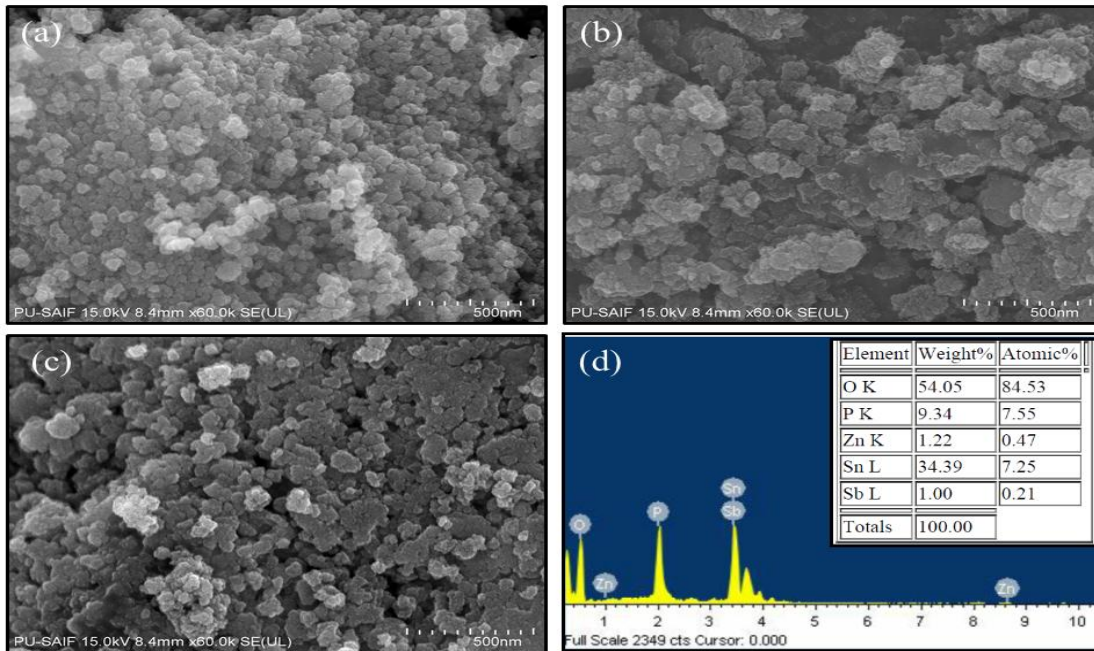


Fig.3. FESEM images of (a) ZnO (b) SnSbP (c) ZnO-SnSbP ion exchanger (d) EDX of ZnO-SnSbP nanocomposite

3.1.4. Transmission Electron Microscopy study

TEM micrographs of ZnO/SnSbP are shown in Fig. 4 at different scale and magnification. In (Fig. 4b) it is assigned that the average particles size of the nanocomposite is ranged between 20-50 nm.

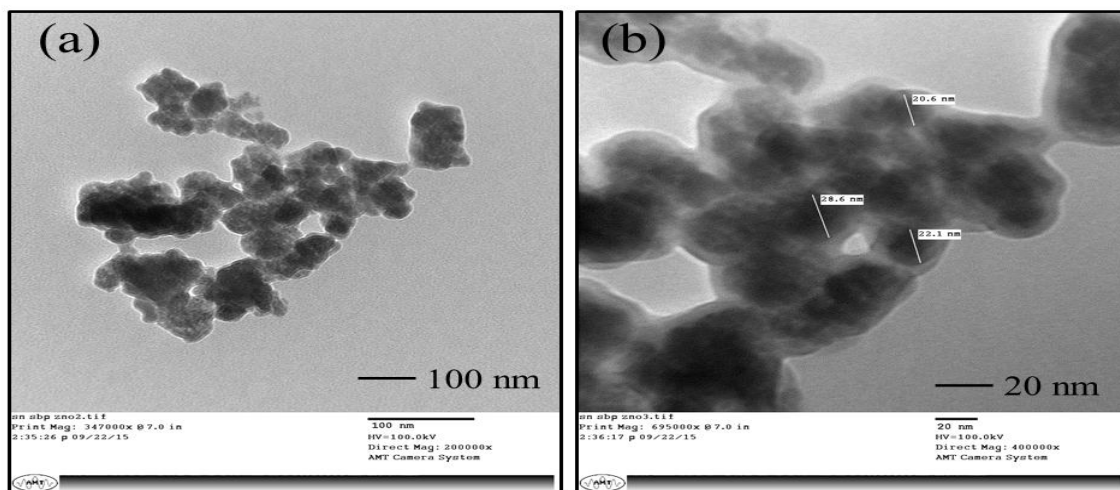


Fig.4 Transmission Electron Microscopy images of (a) (b) ZnO-SnSbPnanocomposite

3.2. Photocatalytic degradation of ZnO/SnSbP Nano composite

The photocatalytic degradation of Methylene blue (MB) dye using ZnO-SnSbPnanocomposite ion-exchanger is showed in Fig. 5. at valid time intervals. It was noticed that 91.6% of MB dye degraded within four hours (Fig.5). The presence of Zn and Sn (IV) metal ions in ZnO-SnSbPnanocomposite ion exchange material may be feasible

for degradation of MB dye. The electron-hole pair can be generated by metal ions and the formation of free radicals that disturbed the conjugation in the free dye molecules as leading to degradation of dye. The rate of photocatalytic degeneration of methylene blue dye was calculated by Langmuir Hinshelwood model using pseudo first-order kinetics as described below [20]:

$$r = -\frac{dc}{dt} = K_{app} t \quad \dots (3)$$

On integrating the above equation, we get

$$\ln \frac{C_0}{C_t} = K_{app} t \quad \dots (4)$$

K_{app} is the apparent rate constant, C_0 is the concentrations of initial dye and C_t is the concentration of dye at different time t . The graph plot between $\ln C_0/C_t$ versus time (t) showed a linear correlation (Fig. 5c) which illustrated that MB dye removed by using ZnO-SnSbPnanocomposite ion exchanger and followed pseudo first-order kinetics [21]. The rate constant value k (0.01268 min^{-1}) was measured from the slope and the correlation coefficient value (R^2) was 0.98905.

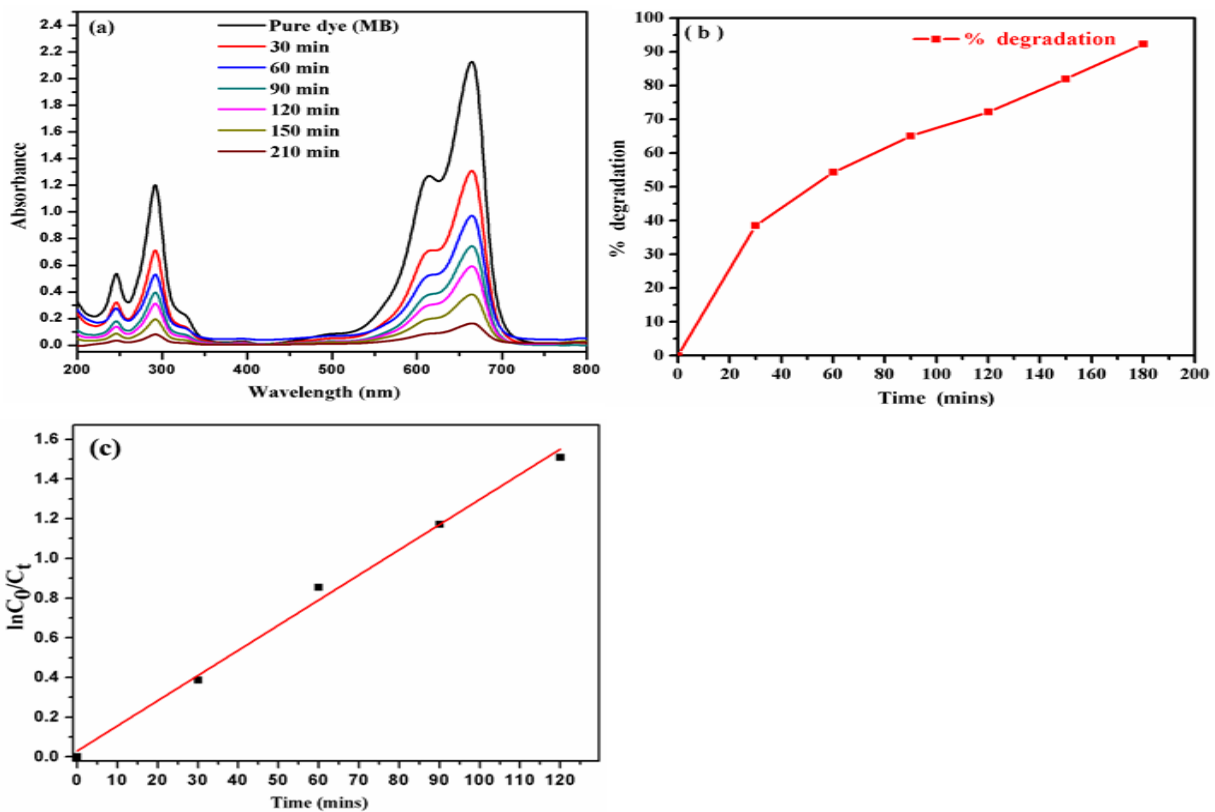


Fig.5. (a) UV–Vis absorption spectra of methylene blue dye for ZnO-SnSbPnanocomposite ion exchanger at various times, (b) percentage degradation of methylene blue dye and (c) kinetics of photocatalytic degradation of methylene blue dye

IVCONCLUSIONS

The ZnO-SnSbPnanocomposite has better ion exchange capacity as the comparison with SnSbP. FTIR and XRD confirm the mixing of ZnO in SnSbP composite. TEM images presented the nanocomposite in nano dimension. The ZnO-SnSbPnanocomposite ion exchanger displayed outstanding photocatalytic degradation property under solar light will be used for the treatment of dye pollutant towards diminishing pollution and environmental protection.

REFERENCES

- [1] R. Cheng, B. Xiang, Y. Li and M. Zhang, Application of dithiocarbamate-modified starch for dyes removal from aqueous solutions, *Journal of Hazardous Materials*, 188(1-3), 2011, 254-260.
- [2] A.T. Paulino, M. R. Guilherme, A.V. Reis, G.M. Campese, E.C. Muniz and J. Nozaki, Removal of methylene blue dye from aqueous media using superabsorbent hydrogel supported on modified polysaccharide. *Journal of Colloid and Interface Science*, 301(1), 2006, 55-62.
- [3] V. K. Gupta, D. Pathania, N. C. Kothiyal and G. Sharma, Polyaniline zirconium (IV) silicophosphate nanocomposite for remediation of methylene blue dye from waste water, *Journal of Molecular Liquids*, 190, 2014, 139-145.
- [4] M.I. Khan, S. Akhtar, S. Zafar, A. Shaheen, M. A. Khan, R. Luque and A. U. Rehman, Removal of Congo Red from Aqueous Solution by Anion Exchange Membrane (EBTAC): Adsorption Kinetics and thermodynamics, *Materials*, 8(7), 2015, 4147-4161.
- [5] M. Naushad, Surfactant assisted nano-composite cation exchanger: Development, characterization and applications for the removal of toxic Pb^{2+} from aqueous medium, *Chemical Engineering Journal*, 235, 2014, 100-108.
- [6] V.K. Gupta, D. Pathania, S. Agarwal and P. Singh, Adsorption and photocatalytic degradation of methylene blue onto pectin-CuSn nanocomposite under solar light, *Journal of Hazardous Materials*, 243, 2012, 179-186.
- [7] A. Ozer, G. Dursan, Removal of methylene blue from aqueous solution by dehydrated wheat bran carbon, *Journal of Hazardous Materials*, 146 (1-2), 2007, 262-269.
- [8] D. Pathania, G. Sharma and R. Thakur, Pectin @ zirconium (IV) silicophosphate nanocomposite ion exchanger: Photo catalysis, heavy metal separation and antibacterial activity, *Chemical Engineering Journal*, 267, 2015, 235-244.
- [9] V. K. Gupta, G. Sharma, D. Pathania and N.C. Kothiyal, Nanocomposite pectinZr(IV) selenotungstophosphate for adsorption/photocatalytic remediation of methylene blue and malachite green dyes from aqueous system, *Journal of Industrial and Engineering Chemistry*, 21, 2015, 957-964.
- [10] Z.M. Siddiqi, D. Pathania, Titanium(IV) tungstosilicate and titanium(IV) tungstophosphate: two new inorganic ion exchangers, *Journal of Chromatography A*, 987 (1-2), 2003, 147-158.

- [11] P.V. Vyas, P. Ray, S.K. Adhikary, B. G. Shah and R. Rangarajan, Studies of the effect of variation of blend ratio on permselectivity and heterogeneity of ion-exchange membranes, *Journal of Colloid and Interface Science*, 257(1), 2003, 127-134.
- [12] R. K. Nagarale, G. S. Gohil, V. K. Shahi, G. S. Trivedi and R. Rangarajan, Preparation and electrochemical characterization of cation- and anion-exchange/polyaniline composite membranes, *Journal of colloid and Interface Science*, 277 (1), 2004, 162-171.
- [13] V.K. Gupta, D. Pathania, P. Singh, B. S. Rathore and P. Chauhan, Cellulose acetate–zirconium (IV) phosphate nano-composite with enhanced photo-catalytic activity, *Carbohydrate Polymers*, 95(1), 2013, 434-440.
- [14] B.K. Korbahti, K. Artut, C. Geegel and A. Ozer, Electrochemical decolorization of textile dyes and removal of metal ions from textile dye and metal ion binary mixtures, *Chemical Engineering Journal*, 173 (3), 2011, 677-688.
- [15] V.K. Gupta, S. Agarwal, D. Pathania, N. C. Kothiyal and G. Sharma, Use of pectin–thorium (IV) tungstomolybdatenanocomposite for photocatalytic degradation of methylene blue, *Carbohydrate Polymer*, 96 (1), 2013, 277-283.
- [16] S. Liu, H. Sun, S. Liu and S. Wang, Graphene facilitated visible light photodegradation of methylene blue over titanium dioxide photocatalysts, *Chemical Engineering Journal*, 214, 2013, 298–303.
- [17] J. Xu, Y. Ao, D. Fu and C. Yuan, Low-temperature preparation of F-doped TiO₂ film and its photocatalytic activity under solar light, *Applied Surface Science*, 254(10), 2008, 3033-3038.
- [18] M. Mittal, M. Sharma and O.P. Pandey, UV–Visible light induced photocatalytic studies of Cu doped ZnO nanoparticles prepared by co-precipitation method, *Solar Energy*, 110, 2014, 386-397.
- [19] M. Mittal, M. Sharma and O. P. Pandey, Fast and quick degradation properties of doped and capped ZnO nanoparticles under UV–Visible light radiations, *Solar Energy*, 125, 2016, 51-64.
- [20] D. Pathania, M. Thakur and A. K. Mishra, Alginate-Zr(IV) phosphate nanocomposite ion exchanger: Binary separation of heavy metals, photocatalysis and antimicrobial activity, *Journal of Alloys and Compounds*, 701, 2017, 153-162.
- [21] M. Thakur, G. Sharma, T. Ahamad, A. A. Ghafar, D. Pathania and M. Naushad, Efficient photocatalytic degradation of toxic dyes from aqueous environment using gelatin-Zr(IV) phosphate nanocomposite and its antimicrobial activity, *Colloids and Surfaces B: Biointerfaces*, 157, 2017, 456-463.
- [22] H. M. Ismail, A thermoanalytic study of metal acetylacetonates, *Journal of Analytical and Applied Pyrolysis*, 21(1), 1991, 315-326.
- [23] M. A. Farrukh, B.T. Heng and R. Adnan, Surfactant-controlled aqueous synthesis of SnO₂ nanoparticles via the hydrothermal and conventional heating methods, *Turkish Journal of Chemistry*, 34, 2010, 537-550.
- [24] O. Acarbas, E. Suvaci and A. Dogan, Preparation of nanosized tin oxide (SnO₂) powder by homogeneous precipitation, *Ceramics International*, 33, 2007, 537-542.
- [25] D.L. Pavia, G.M. Lampman, G.S. Kriz and J.R. Vyvyan, *Introduction to Spectroscopy* (Brooks Cole) Infrared spectroscopy: Bond properties and absorption trends Fifth edition, 2001, 18-19.